Vertical excitation energies for ribose and deoxyribose nucleosides

ARTICLE *in* JOURNAL OF COMPUTATIONAL CHEMISTRY · AUGUST 2007

Impact Factor: 3.59 · DOI: 10.1002/jcc.20699 · Source: PubMed

Vertical Excitation Energies for Ribose and Deoxyribose Nucleosides

REMMICK SO,[1] SAMAN ALAVI[2]
[1]Department of Chemistry, Carleton University, Ottawa, Ontario, Canada K1S 5B6
[2]Steacie Institute for Molecular Sciences, National Research Council of Canada, Ottawa, Ontario, Canada K1A 0R6

Received 28 November 2005; Accepted 18 January 2006
DOI 10.1002/jcc.20699
Published online in Wiley InterScience (www.interscience.wiley.com).

Abstract: Vertical excitation energies for DNA and RNA nucleosides are determined with electron structure calculations using the time-dependent density functional theory (TDDFT) method at the B3LYP/6-311++G(*d*,*p*) level for nucleoside structures optimized at the same level of theory. The excitation energies and state assignments are verified using B3LYP/aug-cc-pVDZ level calculations. The nature of the first four excited states of the nucleosides are studied and compared with those of isolated bases. The lowest nπ^* and $\pi\pi^*$ transitions in the nucleoside remain localized on the aromatic rings of the base moiety. New low-energy nπ^* and $\pi\sigma^*$ transitions are introduced in the nucleosides as a result of bonding to the ribose and deoxyribose molecules. The effect on the low-lying excited state transitions of the binding to phosphate groups at the 5′- and 3′,5′-hydroxyl sites of the uracil ribose nucleoside are also studied. Some implications of these calculations on the de-excitation dynamics of nucleic acids are discussed.

 J Comput Chem 00: 000–000, 2007

Key words: nucleosides; vertical excitation energies; TDDFT method; excited electronic states; nucleic acid bases; electronic de-excitation of DNA

Introduction

The purine and pyrimidine nucleic acid bases adsorb strongly in the 200–300 nm UV range, but the ultrafast radiationless decay of excited electronic states minimizes radiation damage and enhances the photostability of DNA and RNA molecules. The subpicosecond quenching of the electronic excitation energy by nonradiative processes provides the DNA and RNA molecule with a high degree of photostabitity. The nature and energies of the purine and pyrimidine excited electronic states determine the subsequent relaxation dynamics and have been the subject of many experimental and theoretical studies.[1]

The first few vertical electronic singlet state excitations for DNA and RNA bases in the gas phase and solution are well studied and lie about 5 eV above the ground state minimum. The low energy nπ^*, $\pi\pi^*$, and $\pi\sigma^*$ transitions are localized on the heteroatomic aromatic ring systems of the bases and form conical intersections with the ground electronic state. The vertical excitation energies of the bases have been calculated at different levels of theory and for the low-lying vertical excitation energies, the TDDFT method at the B3LYP level has been shown to give correct experimental vertical ordering of the states.[1,2] Ref. 1 gives a review of experimental measurements and calculations of vertical excitation energies up to 2004. Shukla and Leszczynski[2] show that for low-lying levels of nucleic acid bases the 6-311++G(*d*,*p*) basis set gives converged vertical excitation energies with basis sets as large as the 6-311(3+,3+)G(*df*,*pd*). Higher excited state levels can have Rydberg ($\pi\sigma^*$) contamination and require more diffuse basis sets for their accurate characterization.[2]

A number of different mechanisms have been proposed for the radiationless decay of the excited nucleic acid bases. In free nucleic acid bases, the lowest $\pi\sigma^*$ state is thought to play an important role in the radiationless decay of the electronic excitations by providing a pathway for the pre-dissociation of $\pi\pi^*$ and nπ^* states and also a conical intersection with the S_0 state.[3] A different mechanism for radiationless decay based on the presence of a conical intersection of the nπ^* S_1 state with the ground electronic level has also been proposed for adenine.[4] An alternative de-excitation mechanism for cytosine, thymine, and adenine[4–6] involves a conical intersection between the first $\pi\pi^*$ S_1 excited state and the ground electron state. The higher electronic levels are not directly involved in this de-excitation mechanism.

This article contains supplementary material available via the Internet at http://www.interscience.wiley.com/jpages/0192-8651/suppmat

Correspondence to: S. Alavi; e-mail: saman.alavi@nrc-cnrc.gc.ca

Contract/grant sponsor: National Research Council of Canada

In this study we perform theoretical calculations on the vertical excitation energies of the DNA and RNA nucleosides. Deoxyribose or ribose sugar molecules are attached to the N1 or N9 atoms of the pyrimidines and purines, respectively, at the site of the 1′ carbon atom of the sugars. Compared with the isolated bases, the nucleosides have the furanose oxygen and two (in deoxyribose) or three (in ribose) hydroxyl oxygen atoms in configurations in proximity to the purine and pyrimidine rings. These substituents can give rise to new $n\pi^*$ and $\pi\sigma^*$ transitions, which in turn may affect the de-excitation pathways of the electronically excited nucleosides. The effect on the vertical excitation energies of phosphate substitutions at the 3′ and 5′ hydroxyl groups of the sugar is also studied for the uracil ribonucleoside. To facilitate the comparison of the energy level structure and vertical excitation energies of the nucleosides with those of the isolated bases, the vertical excitation energies are calculated with the TDDFT method at the B3LYP/6-311++G(*d, p*) level, which is identical to the level of theory used for the isolated bases.[2,7]

A discussion of theoretical methods is presented in the following section. The values of the first four vertical excitation energies and a description of the nature of the nucleoside excited states are then presented. The paper concludes with a discussion of possible effects of binding to the sugar molecule on nucleoside electronic relaxation mechanisms.

Theoretical Methods

Structures of the uracil, thymine, cytosine, adenine, and guanine nucleosides were optimized by energy minimization with the Gaussian 98 suite of programs.[8] Density functional theory at the B3LYP/6-311++(*d,p*) level[9] was used for optimizations of the geometries that mimic the nucleoside structures in DNA and RNA strands. Normal mode analysis was performed on the optimized structures to verify that they are stable ground-state structures.

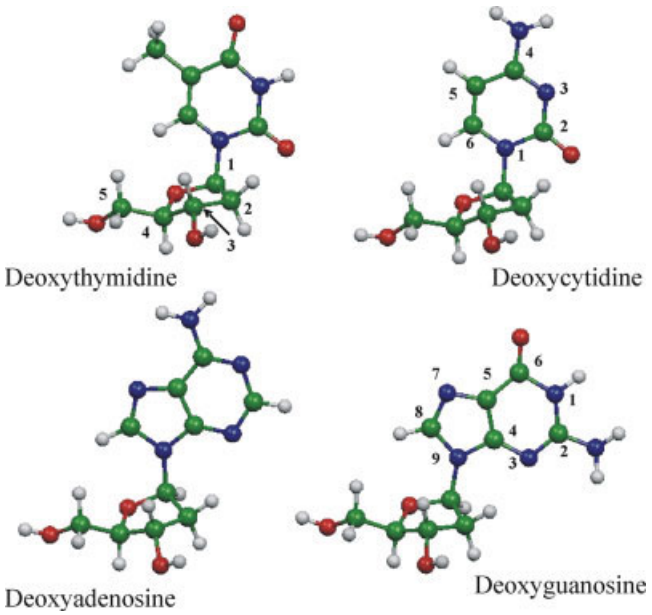

Figure 1. The optimized structures of the deoxyribose nucleosides obtained from calculations at the B3LYP/6-311++G(d,p) level of theory. The numbering of the five carbon atoms of the deoxyribose is shown for the thymidine nucleoside. The numberings of the purine and pyrimidine ring atoms are also shown. The carbon atoms are shown in green, nitrogen in blue, oxygen in red, and hydrogen in white. [Color figure can be viewed in the online issue, which is available at www.interscience.wiley.com.]

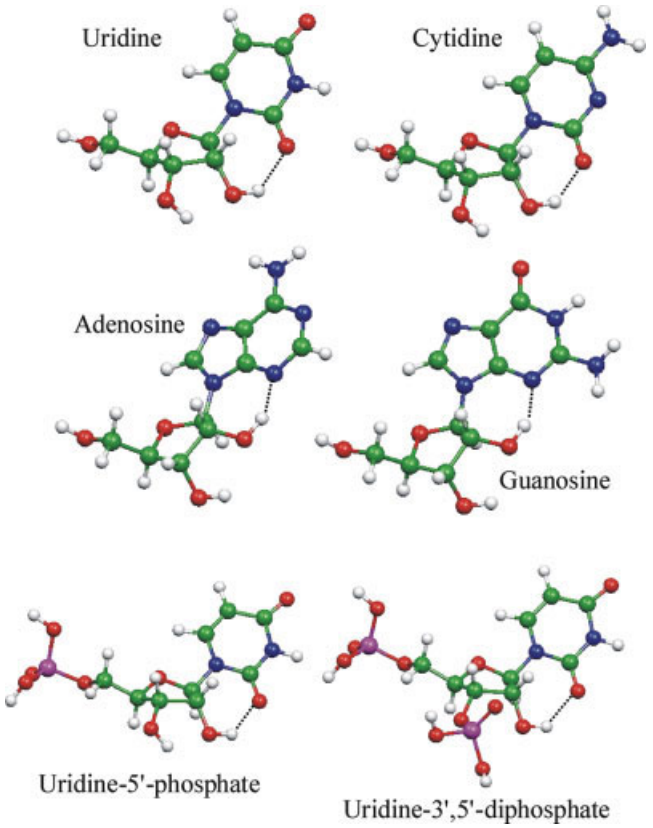

Figure 2. The optimized structures of the ribose nucleosides, uridine-5′-phosphate and uridine-3′,5′-diphosphate obtained from B3LYP/6-311++G(d,p) calculations. Hydrogen bonding of the ribose 2′-OH group with the pyrimidine carbonyl oxygen or purine ring nitrogen is shown. The carbon atoms are shown in green, nitrogen in blue, oxygen in red, and hydrogen in white. [Color figure can be viewed in the online issue, which is available at www.interscience.wiley.com.]

The first four vertical excitation energies and excited state assignments of the nucleosides were determined with the time-dependent density functional theory (TDDFT)[10,11] method at the B3LYP/6-311++G(*d,p*) level of theory. The energies and excited state assignments have also been checked with the Dunning correlation consistent aug-cc-pDVZ basis set.[12,13] This level of theory was recently tested with isolated bases and model nucleoside compounds and gives qualitatively consistent values for vertical excitation energies when compared with spectroscopic data and previous theoretical work.[1,2,7] The TDDFT calculations on the vertical excitation energies of the isolated bases at this level of theory show good agreement with experimentally measured bands for the allowed $\pi\pi^*$ transitions[7] and therefore

Table 1. The first four vertical excitation energies (eV) along with their assignments and oscillator strengths for isolated pyrimidine and purine bases.

Base	Transition[a]	Energy[a]	Description
Ur	$n_{H-1}\pi^*_L$	4.68 (0.000)	[O2,N3,O4]
	$\pi_H\pi^*_L$	5.18 (0.132)	
	$\pi_H\sigma^*_{L+1}$	5.69 (0.002)	{N1-H1}
	$n_{H-3}\pi^*_L - n_{H-1}\pi^*_{L+2}$	5.80 (0.000)	[O2,O4],[O2,N3,O4]
Th	$n_{H-1}\pi^*_L$	4.75 (0.000)	[O2,N3,O4]
	$\pi_H\pi^*_L$	4.99 (0.137)	
	$\pi_H\sigma^*_{L+1}$	5.45 (0.000)	{N1-H1}
	$n_{H-3}\pi^*_L$	5.86 (0.000)	[O2,O4]
Cy	$\pi_H\pi^*_L$	4.64 (0.043)	
	$n_{H-1}\pi^*_L$	4.77 (0.001)	[O2]
	$n_{H-3}\pi^*_L$	5.11 (0.001)	[N3]
	$\pi_H\sigma^*_{L+1}$	5.23 (0.004)	{N4-H4}
Ad	$n_{H-1}\pi^*_L$	4.93 (0.001)	[N1,N3]
	$\pi_H\pi^*_L$	4.99 (0.204)	
	$\pi_H\sigma^*_{L+1}$	5.23 (0.006)	{N9-H9}
	$\pi_H\pi^*_{L+2} - \pi_{H-2}\pi^*_L$	5.25 (0.042)	
Gu	$\pi_H\pi^*_L$	4.60 (0.021)	
	$\pi_H\pi^*_{L+1}$	4.87 (0.135)	{N9-H9}
	$\pi_H\sigma^*_{L+3}$	5.05 (0.007)	
	$\pi_H\pi^*_{L+2}$	5.21 (0.231)	

The transitions are described in terms of the nature of the initial and final states and major contributing levels to these states. The major contributing nonbonded n-state electrons which are excited are shown in brackets. The bonds making the largest contribution to antibonding σ^* states are shown with curly brackets. The labeling of the atoms is given in Figure 1.

[a]Calculations performed with the TDDFT method and the B3LYP/6-311++G(d,p) level of theory on geometries optimized at the same level.

this level was chosen for the calculations of the nucleosides and nucleotides.

Results and Discussion

The optimized deoxyribose and ribose nucleosides are shown in Figures 1 and 2, respectively, and the coordinates of the optimized structures of the nucleosides are given in the Supplementary Materials section. The numbering of the carbons in the ribose (with primes) and the numbering of the atoms in the pyrimidines and purines are shown in Figure 1. The optimized structures of the ribose nucleosides (Fig. 2) show that the 2′-OH group forms an intramolecular hydrogen bond with the pyrimidine C2 carbonyl oxygen (in uracil and cytosine) or to the purine N3 atom (in adenine and guanine).

The first four vertical excitation energies for the isolated bases along with their assignments were previously determined using TDDFT calculations at the B3LYP/6-311++G(*d,p*) level and are reproduced in Table1.[1,2,7] The highest contributing state (states) to each transition and the nature of the nonbonded "*n*" states (in square brackets) and σ^* states (in curly brackets) are given. In complex molecules (such as the nucleosides) the designation of states as n, σ, or π is a useful approximation. These calculated vertical excitation energies compare well with available experimental data,[1,2] previous TDDFT[1,2,7] and multireference configuration interaction DFT (MRCI/DFT)[4] theoretical calculations.

The first four vertical excitation energies for deoxyribo- and ribonucleosides from B3LYP/6-311++G(*d,p*) calculations are given in Tables2 and3, respectively. Similar results for B3LYP/aug-cc-pVDZ calculations are given in the Supplementary Materials. The highest contributing state to each transition and nature of the site of nonbonded states (in square brackets) and σ^* states (in curly brackets) are also provided. The correlations of each nucleoside excited states with the corresponding isolated base excited states and vertical excitation energies are shown in Figures 3–7.

A comparison of the vertical excitation energies of the isolated bases with those of the deoxyribose and ribose nucleosides shows that the vertical excitation energies of the lowest $\pi\pi^*$ transitions generally change by $\approx$0.1 eV as a result of binding to the sugar molecules. In the deoxyribonucleosides (Table 2), the lowest lying $n\pi^*$ states are not changed significantly in comparison with the isolated bases. In the ribonucleosides, hydrogen bonding of the 2′-OH group of the ribose ring with the C2 carbonyl oxygen (pyrimidines) or the N3 purine ring nitrogen atoms stabilizes the nonbonded electrons on these atoms and a causes a blue shift in the lowest lying $n\pi^*$ transitions. For the pyrimidines, the relative order of the first two states is not changed as a result of binding to the sugar groups. The third and fourth vertical excitations for the pyrimidine nucleosides have substantial contributions from the ribose states. Sugar furanose oxygen and OH groups contribute nonbonded electrons in

Table 2. The calculated vertical excitation assignments and energies (eV) for deoxyribose nucleosides.

Base	Transition[a]	Energy[a]	Description
ThdRib	$n_{H-1}\pi_L^*$	4.77 (0.006)	[th O,N]
	$\pi_H\pi_L^*$	4.87 (0.211)	
	$\pi_H\sigma_{L+1}^*$	5.35 (0.004)	{3′-OH}
	$\pi_H\sigma_{L+2}^*$	5.59 (0.002)	{5′-OH}
CydRib	$\pi_H\pi_L^*$	4.67 (0.102)	
	$n_{H-1}\pi_L^* - n_{H-2}\pi_L^*$	4.87 (0.002)	[cy O,N],[cy O,N]
	$n_{H-3}\pi_L^*$	5.22 (0.001)	[cy O,N]
	$\pi_H\sigma_{L+1}^*$	5.23 (0.005)	{mixed}
AddRib	$\pi_H\pi_L^* + \pi_{H-1}\pi_L^*$	4.90 (0.172)	
	$n_{H-1}\pi_L^*$	4.95 (0.048)	
	$\pi_H\pi_{L+3}^* - \pi_H\sigma_{L+1}^*$	5.15 (0.038)	{3′-OH}
	$\pi_H\sigma_{L+1}^*$	5.25 (0.025)	{3′-OH}
GudRib	$\pi_H\pi_L^*$	4.48 (0.017)	
	$\pi_H\pi_{L+1}^* + \pi_H\pi_{L+2}^*$	4.75 (0.125)	
	$\pi_H\pi_{L+2}^* - \pi_H\pi_{L+1}^*$	4.86 (0.017)	
	$\pi_H\pi_{L+3}^*$	5.14 (0.190)	

The major contributing non-bonded n-state electrons which are excited are shown in brackets. The bonds making the largest contribution to anti-bonding σ^* states are shown with curly brackets. The labeling of the atoms is given in Figure 1.

[a]Calculations performed with the TDDFT method and the B3LYP/6-311++G(d,p) level of theory on geometries optimized at the same level.

Table 3. The calculated vertical excitation assignments and energies (eV) for ribose nucleosides.

Base	Transition[a]	Energy[a]	Description
UrRib	$n_{H-1}\pi_L^*$	4.75 (0.001)	[ur O,N]
	$\pi_H\pi_L^*$	5.04 (0.218)	
	$n_{H-2}\pi_L^*$	5.59 (0.001)	[ether O, 3′-OH]
	$n_{H-3}\pi_L^*-n_{H-4}\pi_L^*$	5.85 (0.000)	[2′-OH,3′-OH,5′-OH], [ether,2′-OH,5′-OH]
CyRib	$\pi_H\pi_L^*$	4.75 (0.113)	
	$n_{H-3}\pi_L^*+ n_{H-4}\pi_L^*$	5.05 (0.003)	[cy O,N],[cy O,N, ether O,2′-OH,5′-OH]
	$n_{H-1}\pi_L^*-n_{H-4}\pi_L^*-n_{H-5}\pi_L^*$	5.34 (0.052)	[cy O,N],2×[cy O,N, ether O,2′-OH,5′-OH]
	$n_{H-3}\pi_L^*-n_{H-1}\pi_L^*-n_{H-5}\pi_L^*$	5.44 (0.067)	2× [cy O,N],[cy O,N, ether O,2′-OH,5′-OH]
AdRib	$\pi_H\pi_L^*$	4.93 (0.210)	
	$n_{H-1}\pi_L^*+ n_{H-2}\pi_L^*$	5.04 (0.008)	
	$\pi_H\pi_{L+1}^*$	5.20 (0.067)	
	$\pi_H\sigma_{L+3}^*$	5.46 (0.008)	{NH_2}
GuRib	$\pi_H\sigma_L^*$	4.58 (0.028)	{NH_2}
	$\pi_H\pi_{L+1}^*$	4.78 (0.118)	
	$\pi_H\pi_{L+2}^*$	5.16 (0.180)	
	$n_{H-2}\pi_{L+2}^*$	5.31 (0.000)	[O,N7]

The major contributing nonbonded n-state electrons that are excited are shown in brackets. The bonds making the largest contribution to anti-bonding σ^* states are shown with curly brackets. The labeling of the atoms is given in Figure 1.

[a] Calculations performed with the TDDFT method and the B3LYP/6-311++G(d,p) level of theory on geometries optimized at the same level.

$n\pi^*$ transitions and can also accept electrons in σ^* states and there is considerable mixing of base and ribose states in the higher excitations of the pyrimidine nucleosides. The results for each individual nucleoside are discussed briefly below.

Binding to ribose and deoxyribose enhances the oscillator strengths of pyrimidines. Increases of about 50% in oscillator strength of the lowest-lying $\pi\pi^*$ transitions are observed in the pyrimidines while purine nucleosides are not affected to a large extent.

Uridine and Thymidine

The lowest-lying states in isolated uracil and thymine and their nucleosides are the $n\pi^*$ states. For both nucleosides, the lowest $\pi\pi^*$ state (S_2) is red-shifted with respect to the isolated base, therefore decreasing the gap between the first and second excited states from about 0.5 eV in uracil to 0.3 eV in uridine and from 0.3 eV in thymine to 0.1 eV in deoxythymidine. The nature of the S_3 and S_4 states in the nucleosides differs from those in the isolated bases.

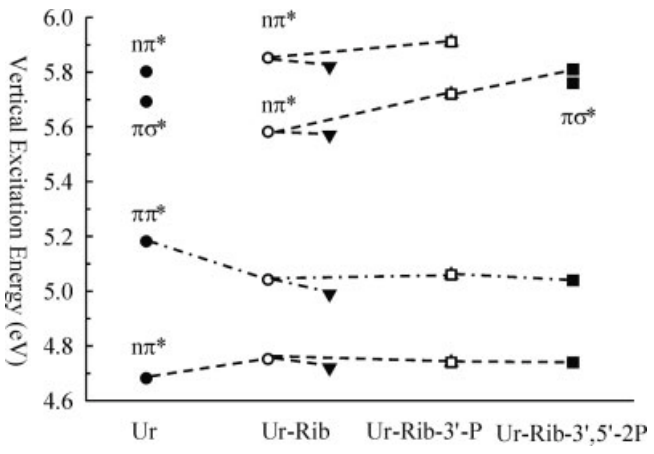

Figure 3. The vertical excitation energies for uracil (●) and uridine at the B3LYP/6-311++G(d,p) level (○) and B3LYP/aug-cc-pVDZ level (▼) from TDDFT calculations. The vertical excitation energies of uridine-3′-phosphate (□) and uridine-3′,5′-diphosphate (■) are also given. Correlations among similar states are shown by connecting them with lines.

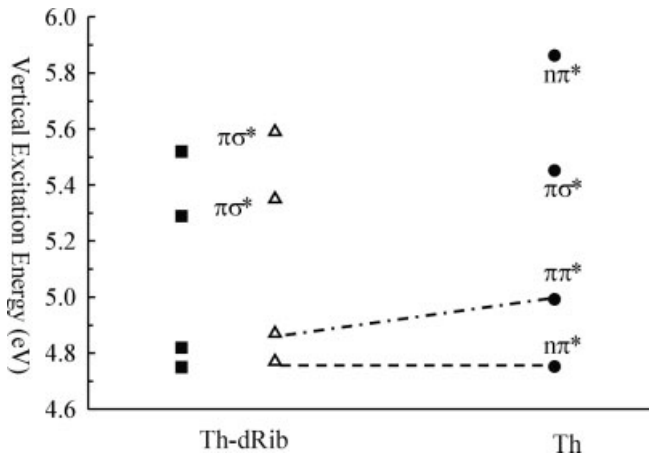

Figure 4. The vertical excitation energies for thymine and the deoxyribose nucleosides from TDDFT calculations at the B3LYP/6-311++G(d,p) level of theory. The B3LYP/aug-cc-pVDZ vertical excitation energies (full symbols) are also given for the nucleosides.

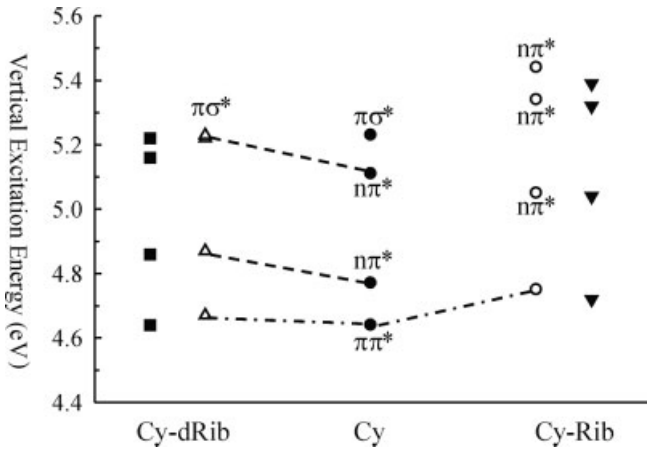

Figure 5. The vertical excitation energies for cytosine and the DNA and RNA nucleosides from TDDFT calculations at the B3LYP/6-311++G(d,p) level of theory. The B3LYP/aug-cc-pVDZ vertical excitation energies (full symbols) are also given for the nucleosides.

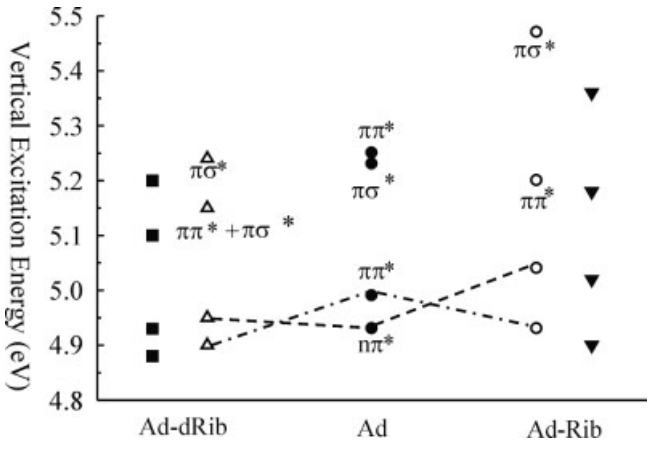

Figure 6. The vertical excitation energies for adenine and its nucleosides from TDDFT calculations at the B3LYP/6-311++G(d,p) level of theory. The B3LYP/aug-cc-pVDZ vertical excitation energies (full symbols) are also given for the nucleosides.

Cytidine

The lowest excited S_1 states for cytosine, cytidine, and deoxycytidine are similar $\pi\pi^*$ states. The closely spaced $n\pi^*$ S_2 state is blue shifted in cytidine and deoxycytidine, therefore slightly increasing the $\pi\pi^*$ to $n\pi^*$ gap in comparison to the value calculated in isolated cytosine. The higher excited state levels of deoxycytidine are similar to those of cytosine, but the S_3 $n\pi^*$ state is blue shifted and is almost degenerate with a $\pi\sigma^*$ state. In cytidine, the $n\pi^*$ excitations have significant mixing of levels. Nonbonded electrons from both the base and the sugar oxygen groups contribute to these $n\pi^*$ states (see Table 3).

Adenosine and Guanosine

For isolated adenine the $n\pi^*$ excitation is the lowest energy transition with a $\pi\pi^*$ transition spaced close in energy. The order of these two transitions is reversed in the adenosine nucleosides. This can be partially due to the blue shift of the $n\pi^*$ excitation caused by hydrogen bonding of the ribose 2′-OH group with the N1 nitrogen of the six-member ring in adenine A similar reversal of the S_1 and S_2 states was seen in the adenine model nucleoside compound. The isolated guanine and deoxyguanosine nucleoside have a $\pi\pi^*$ transition as the lowest energy excitation, while the guanidine nucleoside has a $\pi\sigma^*$ transition localized on the 3′-OH group. In deoxyguanosine, the $\pi\pi^*$ states are red shifted in comparison with the free base. There is also a considerable amount of state mixing between the π-states in this nucleoside.

Nucleotides

The 5′-phosphate ester and 3′,5′-diphosphate ester of uridine are shown in Figure 2 and the vertical excitation energies are given in Table4 and shown in Figure 3. The first two $n\pi^*$ and $\pi\pi^*$ excited state transitions are not perturbed greatly as a result of attachment to the phosphate group. However, the third and fourth excited states are blue shifted in comparison with uridine. The diphosphate has a $\pi\sigma^*$ transition as S_3 which involves σ^* orbitals centered on the phosphate OH groups.

To explicitly determine de-excitation pathways, the energy minima of the excited electronic levels must be determined along with the location of conical intersections between these levels and the ground electronic state. A mechanism has been proposed for the radiationless electronic relaxation of free nucleic acid bases in which the $\pi\sigma^*$ states provide a pathway for the predissociation of $\pi\pi^*$ and $n\pi^*$ states and also a conical intersection with the S_0 state.[3] A different mechanism for radiationless decay of adenine is based on the presence of a conical intersection of the $n\pi^*$ S_1 state with the ground electronic level.[4] In both mechanisms, the low-lying excited states and their neighboring states leads to the form conical intersections which thus effect the de-excitation mechanisms. In this study, it is seen that the

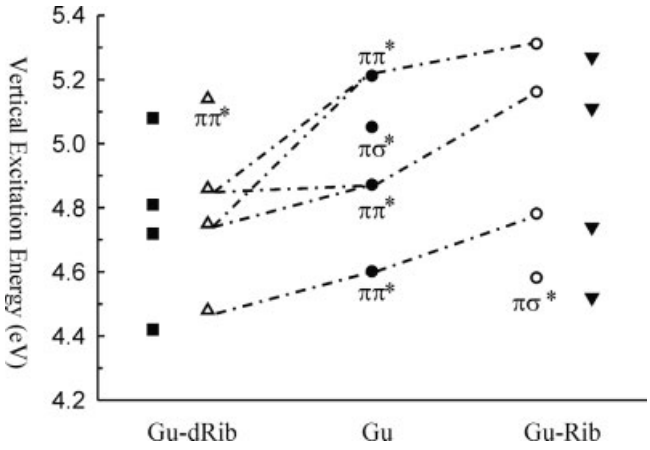

Figure 7. The vertical excitation energies for guanine and its nucleosides from TDDFT calculations at the B3LYP/6-311++G(d,p) level of theory. The B3LYP/aug-cc-pVDZ vertical excitation energies (full symbols) are also given for the nucleosides.

Table 4. The calculated vertical excitation assignments and energies (eV) for uridine 5′-phosphate and uridine-3′,5′-diphosphate.

Base	Transition[a]	Energy[a]	Description
UrRib-5′-phosphate	$n_{H-1}\pi_L^*$	4.75 (0.000)	[ur O,N]
	$\pi_H\pi_L^*$	5.06 (0.218)	
	$n_{H-2}\pi_L^*$	5.72 (0.002)	[ether O, 3′-OH]
	$n_{H-1}\pi_{L+2}^*+n_{H-3}\pi_L^*$	5.91 (0.001)	[ur O,N], [ether O, 2′-OH]
UrRib-3′,5′-diphosphate	$n_{H-1}\pi_L^*$	4.74 (0.000)	[ur O,N]
	$\pi_H\pi_L^*$	5.04 (0.222)	
	$\pi_H\sigma_{L+1}^*$	5.76 (0.001)	{Phosphate-OH}
	$n_{H-2}\pi_L^*$	5.81 (0.000)	[ether O, 2′-OH]

The major contributing nonbonded n-state electrons that are excited are shown in brackets. The bonds making the largest contribution to anti-bonding σ^* states are shown with curly brackets. The labeling of the atoms is given in Figure 1.

[a]Calculations performed with the TDDFT method and the B3LYP/6-311++G(d,p) level of theory on geometries optimized at the same level.

formation of the glycosidic bond between the bases and sugar and the formation of nucleosides and nucleotides mostly affect the third and fourth lowest-lying excited states. If these higher levels participate in the de-excitation mechanism, different electronic relaxation mechanisms may operate in the nucleosides and the isolated bases. A third set of mechanisms have been suggested for cytosine with CASPT2[5] and CR-EOM-CCSD(T)[6] (with excited state geometries determined by CIS calculations) calculations for cytosine and DFT/MRCI[4] and CASSCF[3,14] calculations for adenine. The de-excitation mechanisms of refs. 4–6 involve a conical intersection between the first $\pi\pi^*$ S_1 excited state and the ground electron state. The $\pi\pi^*$ excitations in refs. 3 and 5 both involve out-of-plane deformations of the 6-membered rings of cytosine and adenine. In cytosine the C5 and C6 atoms are displaced out of the plane of the other ring atoms and the excited state has biradical character.[6] In this mechanism, the ring distortion occurs away from the C2N3C4 sites, which are hydrogen bonded to the complementary base pair in DNA, and therefore will not affect the hydrogen bonding of the helical strands. Higher electronic levels are not directly involved in this mechanism. In adenine, the $\pi\pi^*$ excitation is considered to primarily cause a ring deformation at the C2N3 sites.[4] The conical intersection of this excited state with the ground potential energy surface causes a rapid funneling of electronic excitations to the ground state. Once again, the site of hydrogen bonding of adenine (N1 and C6 atoms) to the complementary base pair in the helix will not be disrupted in the electronic excitation.

For the cytosine, uracil, and thymine nucleosides, the nature of the first excited $\pi\pi^*$ state and its relation to the close-lying $n\pi^*$ state are not qualitatively affected by the bonding to the ribose group. In these cases, the electronic relaxation mechanisms in the isolated bases and nucleosides can be expected to be similar. In the case of adenosine, the order of the $\pi\pi^*$ S_1 and $n\pi^*$ S_2 excited states is reverse that of the isolated adenine base. This could lead to a difference in the electronic relaxation mechanism in the adenine nucleoside and the isolated adenine base. The S_1 $\pi\sigma^*$ state in guanosine may also lead to a qualitatively different relaxation mechanism for this nucleoside and the isolated guanine base. Further mechanistic studies are required to clarify these points.

The involvement of the low-lying aromatic ring excited state $\pi\pi^*$ levels in the electronic ultrafast relaxation mechanism raises the intriguing possibility that the purine and pyrimidine bases were biologically selected to incorporate the properties discussed earlier, i.e., they are aromatic systems which are readily excited into biradical $\pi\pi^*$ states that are nonplanar. The ring deformation provides a fast de-excitation mechanism, which at the same time does not affect the hydrogen bonding to the complementary base, thus information retention in the DNA chain is not disrupted and also does not affect the glycosidic bonding of the base to the sugar molecule.

The ordering of the first two $\pi\pi^*$ and $n\pi^*$ vertical excitation energies for the model nucleosides consisting of nucleic acid bases bound with glycosidic bonds to 1-methoxy-2-ethanol and 1-methoxypropane[7] is generally consistent with the calculated values of the vertical excitation energies for the DNA and RNA nucleosides given in this work. As in the case of the nucleosides, the first two vertical excitations remain localized on the aromatic rings of the bases. The ordering and nature of the higher excited states in the model nucleosides differ from those of DNA and RNA nucleosides and the isolated bases. The different nonbonding orbitals on the ethers in the model nucleosides when compared with the sugar molecules in the DNA and RNA nucleosides will lead to different higher-lying vertical excited states. This can be seen by comparing Figures 3–7 of the present work with Figures 6–10 of ref. 7.

Conclusions

The accuracy of the vertical excitation energies of the nucleosides at the B3LYP/6-311++G(*d*,*p*) level were partially verified by calculations using the same structures but with the augmented correlation-consistent polarized double-zeta basis set of Dunning[12] [B3LYP/aug-cc-pVDZ//B3LYP/6-311++G(*d*,*p*)], which are given in the Supporting Material. Similar calculations with TDDFT

method and other functionals and basis sets and also DFT/MRCI[15] or CASSCF/CASPT2 calculations in the future can provide further verification of the conclusions of this work.

The binding of sugar molecules to isolated bases to form nucleosides leaves the first two excited state levels of the base relatively unchanged. The two lowest $\pi\pi^*$ and $n\pi^*$ states are localized on the purine and pyrimidine rings in both the isolated bases and in the nucleosides. The only exception to this observation is the lowest energy transition in the guanidine nucleoside, which is predicted to be a $\pi\sigma^*$ transition. The third and fourth transitions in the isolated bases and nucleosides are different in nature.

Experimentally, relaxation times of the isolated bases and nucleosides are comparable. This may lead to the conclusion that only lowest-lying $\pi\pi^*$ and $n\pi^*$ states, which are relatively unchanged upon nucleoside formation participate primarily in the electronic de-excitation. This remains to be demonstrated by explicit calculation of the de-excitation mechanisms of the isolated bases and nucleosides. Similarly, binding to phosphate groups does not affect the first two low-lying $\pi\pi^*$ and $n\pi^*$ transitions, but drastically changes the nature of the upper two states.

The isolated bases and nucleosides have somewhat similar characteristics in their first two excited states, which include $\pi\pi^*$ and $n\pi^*$ transitions on the base aromatic systems. The fact that all bases and nucleosides have ultrafast electronic relaxation rates may imply that these low-lying two states are involved in the relaxation process. The nature of the higher states is system dependent and it is difficult to envision a uniform mechanism where these diverse states will all lead to uniformly fast de-excitation of the excited electronic states.

References

1. Crespo-Hernández, C. E.; Cohen, B.; Hare, P. M.; Kohler, B. Chem Rev 2004, 104, 1977.
2. Shukla, M. K.; Leszczynski, J. J Comput Chem 2004, 25, 768.
3. Sobolewski, A. J.; Domcke, W. Eur Phys J D 2002, 20, 369.
4. Marian, C. M. J Chem Phys 2005, 122, 103414.
5. Merchán, M.; Serrano-Andés, L. J Am Chem Soc 2003, 125, 8108.
6. Zgierski, M. Z.; Patchkovskii, S.; Lim, E. C. J Chem Phys 2005, 123, 081101.
7. Alavi, S. J Phys Chem A 2005, 109, 9536.
8. Frisch, M. J.; Trucks, G. W.; Schlegel, H. B.; Scuseria, G. E.; Robb, M. A.; Cheeseman, J. R.; Zakrzewski, V. G.; Montgomery, J. A., Jr.; Stratmann, R. E.; Burant, J. C.; Dapprich, S.; Millam, J. M.; Daniels, A. D.; Kudin, K. N.; Strain, M. C.; Farkas, O.; Tomasi, J.; Barone, V.; Cossi, M.; Cammi, R.; Mennucci, B.; Pomelli, C.; Adamo, C.; Clifford, S.; Ochterski, J.; Petersson, G. A.; Ayala, P. Y.; Cui, Q.; Morokuma, K.; Salvador, P.; Dannenberg, J. J.; Malick, D. K.; Rabuck, A. D.; Raghavachari, K.; Foresman, J. B.; Cioslowski, J.; Ortiz, J. V.; Baboul, A. G.; Stefanov, B. B.; Liu, G.; Liashenko, A.; Piskorz, P.; Komaromi, I.; Gomperts, R.; Martin, R. L.; Fox, D. J.; Keith, T.; Al-Laham, M. A.; Peng, C. Y.; Nanayakkara, A.; Challacombe, M.; Gill, P. M. W.; Johnson, B.; Chen, W.; Wong, M. W.; Andres, J. L.; Gonzalez, C.; Head-Gordon, M.; Replogle, E. S.; Pople, J. A.Gaussian 98 (revision A. 7); Gaussian: Pittsburgh, PA, 2001.
9. Becke, A. D. J Chem Phys 1993, 98, 5648.
10. (a) Runge, E.; Gross, E. K. U. Phys Rev Lett 1984, 52, 997, (b) Gross, E. K. U.; Kohn, W. Adv Quantum Chem 1990, 21, 255, (c) Marques, M. A. L.; Gross, E. K. U. Annu Rev Phys Chem 2004, 55, 427.
11. (a) Casida, M. E.; Jamorski, C.; Casida, K. C.; Salahub, D. R. J Chem Phys 1998, 108, 4439, (b) Stratmann, R. E.; Scuseria, G. E.; Frisch, M. J. J Chem Phys 1998, 109, 8218.
12. Dunning, T. H., Jr. J Chem Phys 1990, 90, 1007.
13. (a) Woon, D. E.; Dunning, T. H., Jr. J Chem Phys 1993, 98, 1358 (b) Peterson, K. A.; Woon, D. E.; Dunning, T. H., Jr. J Chem Phys 1994, 100, 7410.
14. Perun, S.; Sobolewski, A. J.; Domcke, W. J Am Chem Soc 2005, 127, 6257.
15. Grimme, S.; Waletzke, M. J Chem Phys 1999, 111, 5645.